Analysis of photoinduced stress distribution in fiber Bragg gratings

A. I. Gusarov

Faculté Polytechnique de Mons, B-7000 Mons, Belgium, and
Studiecentrum voor Kernenergie Centre d'Etude de l'Energie Nucléaire, Belgian Nuclear Research Centre, B-2400 Mol, Belgium

D. B. Doyle

European Space Research and Technology Centre, European Space Agency, 2200 AG Noordwijk, The Netherlands

F. Berghmans

Studiecentrum voor Kernenergie Centre d'Etude de l'Energie Nucléaire, Belgian Nuclear Research Centre, B-2400 Mol, Belgium, and
Laboratory for Photonics, Vrije Universiteit Brussel, B-1050 Brussels, Belgium

O. Deparis

Faculté Polytechnique de Mons, B-7000 Mons, Belgium

Received June 14, 1999

We discuss the analytical expressions that describe the displacement field resulting from the inscription of a Bragg grating in a Ge-doped optical fiber. The equations stem from a phenomenological approach and allow calculation of the induced stresses. Our model provides an efficient tool to analyze the effects of radiation-induced density variations on the properties of fiber Bragg gratings. © 1999 Optical Society of America

OCIS codes: 050.2770, 060.2430, 060.2400, 230.1480.

The fabrication of a fiber Bragg grating (FBG) commonly relies on the change of the refractive index (RI) in Ge-doped silica glass that is induced by exposure to UV radiation. This photosensitivity is ascribed to the generation of radiation defects that correspond to local changes of the glass structure after UV exposure. One model of the photosensitivity that is usually invoked to account for the RI change is the color-center model.[1] The RI change is derived from the induced absorption by use of the Kramers–Kronig relations. Another type of model relates the changes in the RI to structural transformations[2,3] that result in density variations[4,5] and stress increase,[6] or possibly in relaxation of frozen stress.[3] Densification is an experimentally established effect accompanying the grating formation in Ge-doped silica fibers,[4,5] which can explain the high values of the RI change through the photoelastic effect.[7] A quantitative evaluation of the role of density changes in photosensitivity phenomena requires an analysis of the stress distribution induced by a grating inscription. This analysis also allows an understanding of the effect that grating inscription has on the fiber strength to be gained.[8]

A model that reveals the role of UV-induced densification in the formation of index gratings within germanosilicate preform slices was proposed by Poumellec *et al.*[7] Unfortunately, this model is not accurate when applied to FBG's. Recently Chen *et al.* used a finite-element analysis to evaluate stresses caused by photoinduced densification to assess the effect of a Bragg grating inscription on fiber strength.[8] The densification was assumed to be proportional to the UV fluence. The analogy between thermal expansion and UV-induced densification allowed the use of standard finite-element analysis software to compute the stress distribution.

In this Letter we present an approach that allows the analytical calculation of the stress distribution in an optical fiber that results from the inscription of a grating. The structural changes are analyzed on the basis of a set of differential equations that follow from the continuum approximation of the elasticity theory. The fiber symmetry plays an important role in this analysis. We assume that the glass-density change at a given point $\mathbf{r}$ is a function of the absorbed UV-light dose $D(\mathbf{r})$ at that point,

$$\Delta\rho/\rho = -f[D(\mathbf{r})], \tag{1}$$

where the function f is not specified at the moment. The density change can often be approximated by a sublinear (type I grating) dependence.[9] The displacement field $\mathbf{u}$ that is induced by the radiation defects is then described by[10]

$$\mu\nabla^2\mathbf{u} + (\lambda + \mu)\nabla(\nabla \cdot \mathbf{u}) = K\nabla f[D(\mathbf{r})],$$

$$K = \lambda + {}^2/_3\mu, \tag{2}$$

where λ and μ are the Lamé coefficients. We use a cylindrical system of coordinates $\mathbf{r} = (r, \varphi, z)$ with the polar axis (z) directed along the fiber axis. We can represent $\mathbf{u} = \{u_r, u_\varphi, u_z\}$ as $\mathbf{u} = \nabla\Phi + \mathbf{w}$, where Φ and $\mathbf{w}$ are the scalar and the vector potentials, respectively. Substitution of $\mathbf{u}$ in the form of this sum into Eq. (2) gives

$$\nabla[(\lambda + 2\mu)\nabla^2\Phi - Kf(\mathbf{r})] +$$

$$\{\mu\nabla^2\mathbf{w} + (\lambda + \mu)\nabla(\nabla \cdot \mathbf{w})\} = \mathbf{0}. \tag{3}$$

0146-9592/99/191334-03$15.00/0

Equation (3) holds if Φ satisfies the Poisson equation and if the vector potential $\mathbf{w}$ is a solution of the equation corresponding to that part of Eq. (3) between the braces. The boundary conditions for our problem can be derived from the periodicity of the FBG. Let us consider the planes $z = \pm\Lambda/2 \pm k\Lambda$, $k = 0, 1, \ldots$, which correspond to the minima of the UV-radiation intensity. Λ is the grating period. Owing to the translation invariance, the z component of the forces acting from the left-hand side and the right-hand side compensate for each other. Therefore these planes can be considered z clamped (the first boundary condition). The second boundary condition corresponds to the absence of stresses on the free (outer) surface of the fiber.

In a step-index single-mode fiber only the fiber core, of radius R, is photosensitive. For such a fiber the diameter of the core is small in comparison with the inverse absorption coefficient; e.g., the natural absorption coefficient in a silica-fiber core doped with 11-mol.% GeO_2 is $\sim 50\ \mathrm{cm}^{-1}$ at 240 nm.[7] Therefore we assume that the radiation-induced density variation is independent of r within the core and is a function of only z,

$$f(z) = N(z)\Theta(R - r), \tag{4}$$

where $\Theta(x)$ is the step function and $N(z)$ describes the axial distribution of the density variation. Solution of Eq. (3) for any given $N(z)$ results in rather complicated expressions for the potentials. However, for the particular case of sinusoidal modulation,

$$N(z) = \tfrac{1}{2}N_0[1 + b\cos(az)], \qquad a = 2\pi/\Lambda, \tag{5}$$

which corresponds to the absence of saturation, the solution can be significantly simplified. In Eq. (5), N_0 is the relative density modulation amplitude and b is the fringe visibility.

Equation (5) is not suitable for fiber gratings for which high fluences are used for writing. We can, however, consider $f(z)$ in Eq. (1) in terms of a Fourier series with the periodicity of the grating pitch. Only the zero- and the first-order harmonics will contribute to the Bragg wavelength (the peak position and the reflection amplitude). Therefore Eq. (5) is sufficient to describe the effect of the induced stresses on the main optical grating characteristics. Direct substitution shows that the scalar field given by

$$\Phi(r, z) = -\gamma[F(r) + b\cos(az)P(r)],$$

$$\gamma = N_0K/2(\lambda + 2\mu) \tag{6}$$

satisfies the Poisson equation and the first boundary condition. Here

$$P(r) = \begin{cases} a^{-2} - (R/a)I_0(ar)K_1(aR) & r < R \\ (R/a)K_0(ar)I_1(aR) & r > R \end{cases}, \tag{7}$$

$$F(r) = R\int_0^\infty \mathrm{d}\alpha\,\alpha^{-2}J_0(\alpha r)J_1(\alpha R),$$

where J_0, J_1, I_0, I_1, K_0, and K_1 are standard Bessel functions. The solution is angle independent owing to the cylindrical symmetry of the density variation. This solution also shows that the scaling factor for the axial displacements is the grating period and that the radial displacements scale with the core radius.

The second boundary condition can be satisfied by a proper choice of $\mathbf{w}$. However, the stress distribution described by Eqs. (6) and (7) decays rapidly outside the fiber core. For a standard single-mode telecommunication fiber $R_{\mathrm{clad}} \gg R$, and we can neglect the stresses related to the scalar potential solution on the free surface of the fiber. This means that the trivial solution

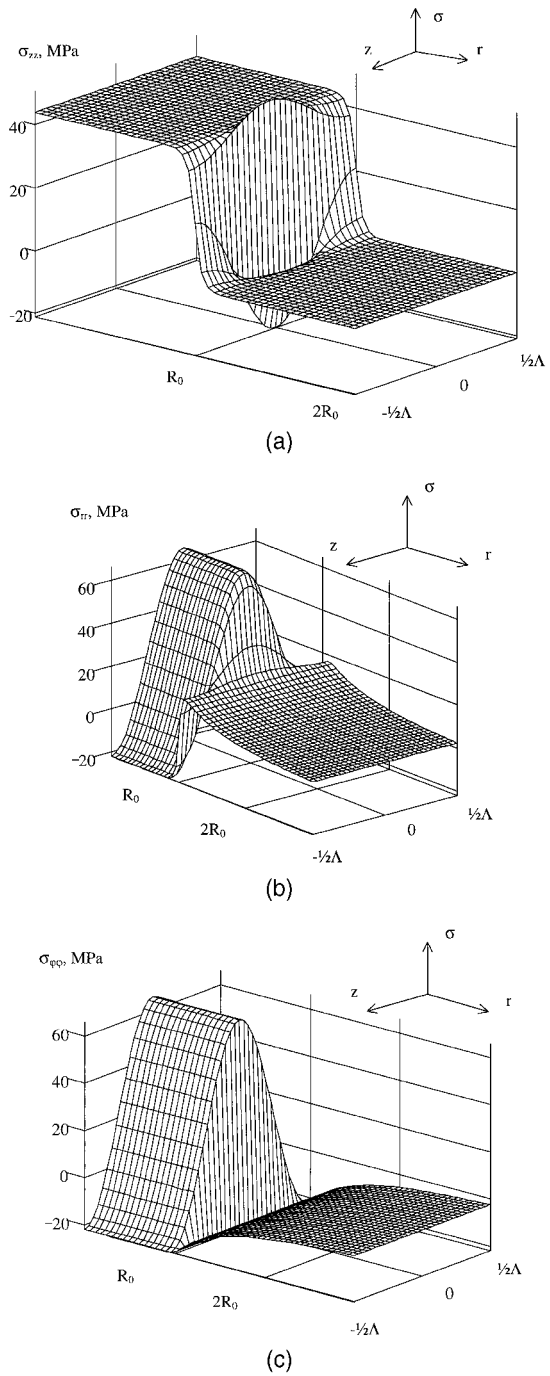

Fig. 1. Computed distribution of the stress induced by a grating inscription with a period of 0.4 μm in a fiber with a 4.0-μm core radius: (a) axial stress $\sigma_{zz}(r, z)$, (b) radial stress $\sigma_{rr}(r, z)$, (c) tangential stress $\sigma_{\varphi\varphi}(r, z)$.

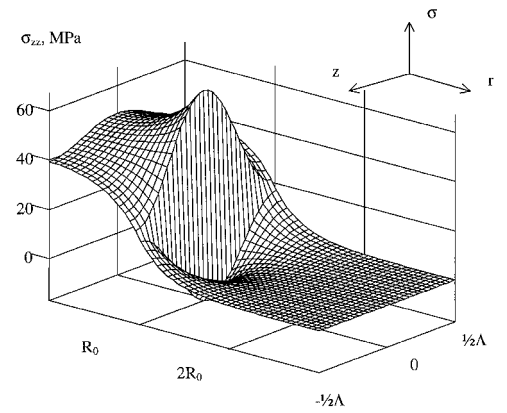

Fig. 2. Computed axial stress distribution $\sigma_{zz}(r, z)$ induced by a grating inscription with a period equal to the fiber-core radius (4.0 μm).

$\mathbf{w} = \mathbf{0}$ fits the problem and that Eqs. (6) and (7) represent the complete solution.

We are now able to evaluate the displacement field, the strain, and the stress distributions, using the standard relations of the elasticity theory. N_0 can be derived from the experimental data reported by Fonjallaz *et al.*[6] in such a way that the maximum of the computed stress fits the experiment. For a RI change of 3.0×10^{-4} the induced stress reported in Ref. 6 ranged from 33 MPa for a fiber with 18-mol.% GeO_2 doping to 62 MPa for a fiber with 9-mol.% GeO_2, corresponding to N_0 in a range from -1.7×10^{-3} to -3.0×10^{-3}. The negative sign of N_0 corresponds to a density increase. It should be noted that the model is equally applicable in the analysis of the effect of glass expansion.[11]

Computed distributions of photoinduced stresses are shown in Fig. 1. The grating period $\Lambda = 0.4$ μm, the core radius $R = 4.0$ μm, $N_0 = -3 \times 10^{-3}$, and $b = 1$. In a thin boundary layer just outside the core the induced axial stress $\sigma_{zz}(r, z)$ is tensile or compressive, depending on the axial position z. In the cladding both $\sigma_{rr}(r, z)$ and $\sigma_{\varphi\varphi}(r, z)$ are nearly independent of the axial position and have opposite signs. Although the scalar potential and its first derivatives (displacements) are continuous everywhere, the axial and the tangential stresses exhibit discontinuity at the core–cladding interface. This discontinuity is related to the assumed sharp boundary between the photosensitive core and the nonsensitive cladding. Inside the core the axial stress component is tensile and also nearly independent of the axial position for $r < 0.8\, R_0$. By contrast, $\sigma_{rr}(r, z)$ and $\sigma_{\varphi\varphi}(r, z)$ are tensile at the maxima of the UV-fringe pattern and compressive at the minima. Such behavior of the stress field is defined by the condition $\Lambda \ll R$, which is typical for FBG's. By way of illustration, Fig. 2 shows the axial stress distribution for the extreme case $\Lambda = R$. Although the qualitative behavior is the same as for $\Lambda \ll R$, the z dependence of variation of the axial stress is more pronounced.

In conclusion, we have developed an approach to computing the stresses induced in a fiber by grating inscription. The elasticity problem was solved analytically, and the components of the stress distribution were computed. Our results are in qualitative agreement with the experimental results of Fonjallaz *et al.*[6] Quantitative comparison is not possible owing to the low spatial resolution of the method used in that experiment. The results of our computations also confirm the conclusion drawn by Chen *et al.*[8] by use of finite-element analysis that major stress variations occur at the core–cladding interface. Compared with the numerical solution, our approach provides an accurate and simple way to compute not only the stresses but also the displacements. In this way we have made available an efficient tool for analyzing the effect of density variations on fiber-grating properties.

O. Deparis is supported by the Inter-University Attraction Pole Program (IAPIV/07) of the Belgian government (SSTC). A. I. Gusarov is indebted to H. G. Limberger for stimulating discussions; his e-mail address is gusarov@telecom.fpms.ac.be.

References

1. D. P. Hand and P. St. J. Russell, Opt. Lett. **15,** 102 (1990).
2. J. P. Bernardin and N. M. Lawandy, Opt. Commun. **79,** 194 (1990).
3. M. G. Sceats, G. R. Atkins, and S. B. Poole, Annu. Rev. Mater. Sci. **23,** 381 (1993).
4. B. Poumellec, P. Guenot, I. Riant, P. Sansonetti, P. Niay, P. Bernage, and J. F. Bayon, Opt. Mater. **4,** 441 (1995).
5. M. Douay, W. X. Xie, T. Taunnay, P. Bernage, P. Niay, P. Cordier, B. Poumellec, L. Dong, J. F. Bayon, H. Poignant, and E. Delevaque, J. Lightwave Technol. **15,** 1329 (1997).
6. P. Y. Fonjallaz, H. G. Limberger, R. P. Salathé, F. Cochet, and B. Leuenberger, Opt. Lett. **20,** 1346 (1995).
7. B. Poumellec, P. Niay, M. Douay, and J. F. Bayon, J. Phys. D **29,** 1842 (1996).
8. S. Chen, B. Liu, J. Sirkis, M. K. Park, and S. Singh, Proc. SPIE **3746,** 478 (1999).
9. J. Albert, B. Malo, K. O. Hill, F. Bilodeau, D. C. Johnson, and S. Thériault, Appl. Phys. Lett. **67,** 3529 (1995).
10. J. D. Eshelby, in *Solid State Physics,* F. Seitz and D. Turnbull, eds. (Academic, New York, 1956), Vol. 3, p. 79.
11. J. Canning and M. Åslund, Opt. Lett. **24,** 463 (1999).